Finite Control Set based Optimized Model Predictive Current Control of Four-leg Shunt Active Power Filter

J.Chelladurai, B.Vinod, J. Joe Brislin

PSG College of Technology, Coimbatore, TamilNadu, India
(e-mail: jcd@eee.psgtech.ac.in)

Abstract: This paper presents a finite control set based Model Predictive Current Control (MPCC) of a four-leg Shunt Active Power Filter (SAPF) to mitigate the current harmonics and to balance a three-phase four-wire system. A four-leg inverter is considered to balance the three-phase current in the distribution system under unbalanced load conditions. The four-leg inverter provides a path for the neutral current to flow on the load side. The instantaneous i_{d_axis}-i_{q_axis} current method is applied to estimate the required compensating current. The squared error based cost function optimization is proposed in the MPCC technique. PID regulators are used in most of the classical current control technique based four-leg SAPF to mitigate the current harmonics and to balance the load current. The proposed SAPF using MPCC technique has the inherent advantage of zero modulation stage and the control part considers only the mathematical model of the system which eliminates the requirement of PID regulator. The performance of the proposed four-leg SAPF using MPCC control strategy is evaluated under different source voltage and load conditions. The simulation results of the proposed system prove that the four-leg SAPF with MPCC is more desirable to have an effective current harmonic compensation and to balance the three-phase four-wire distribution system.

Keywords: Active Filters, Inverters, Harmonics, Predictive Control

1. INTRODUCTION

Power quality has emerged as a major research area of electrical power engineering. The predominant reason for the importance is the increasing use of sophisticated end-use equipments. Single-phase unbalanced loads and non-linear nature of loads like Switched Mode Power Converters, conventional DC power supplies, battery charging circuits and Electric Drives inject harmonics into the power system and pollute the distribution system. Traditionally, harmonic reduction has been done by using passive LC filters. The major disadvantage of using these filters is that it leads to the resonance of the supply at some harmonic frequencies. The harmonic currents and voltages produced by three-phase non-linear loads such as Motor Drives, Rectifiers, and Uninterruptible Power Supplies (UPS) are both positive and negative-sequence harmonics (Enjeti et al., 1994). However, harmonic currents and voltages produced by single-phase non-linear load like, Switch-Mode Power Supplies are third order zero-sequence harmonics. These triplen harmonic currents do not cancel but add up arithmetically at the neutral bus (Quinn et al., 1993). This leads to excessive power loss and it affects system protection.

The active filter techniques using three-leg power converters to compensate the unbalanced load and source is discussed in the literature (Verdelho and Marques, 1997). However, a three-leg power converter is not capable of dealing with zero-sequence components under unbalanced load conditions. In order to avoid the problems caused by unbalanced loads, it is important to have a control over the zero-sequence component. In order to address this issue, normally split DC link capacitors are used. The zero-sequence current path is provided by connecting the neutral point to the midpoint of the two DC link capacitors. This requires large DC link capacitors, and this can be a major limitation of this scheme. A complex control technique is required to avoid voltage unbalance across the DC link capacitors (Ei-Barbari, and Hofmann, 2000). Use of the four-leg inverter topology with its associated control for handling the zero sequence components are discussed in the literature (Singh et al., 1998; Khadkikar et al., 2011). Power quality issues in IT park is discussed in the literature (Joshi et al., 2012).The current control of four-leg converters are used in many applications, such as grid-connected distributed generation systems, shunt active power filters, active front-end rectifiers and electric drives. Various aspects of these four leg converters have been studied in many papers.

The carrier-based Pulse Width Modulation (PWM) and 3D Space Vector Modulation (3DSVM) schemes are widely used for the four-leg inverters (Fernandes et al., 2013; Nguyen-Van Nho et al., 2004). The use of 3DSVM offers many advantages over that of carrier-based PWM, such as good DC link utilization and minimum output distortion. However they require complex modelling and higher computational capacity. In these classical current control techniques conventional PID regulators are used to eliminate the steady state error. Fuzzy logic controller based four-leg SAPF has been addressed by (Acordi et al., 2014). Under parametric variation of the physical system, the THD performance is found to be around 11-12%. To overcome the above

mentioned limitations, this work uses model predictive current controller based active power filter to mitigate the current harmonics and to balance the load current. The model predictive control has the inherent advantage of zero modulation stage and the control part considers only the mathematical model of the line impedance and filter elements. However, there is no comprehensive study on the four leg inverter based SAPF using MPCC scheme.

The instantaneous reactive power theory (Akagi et al., 1984) is used very successfully to design and control the active power filter for three-phase systems. This theory is extended for applications in three-phase four-wire systems (Aredes et al., 1997). The instantaneous reactive power theory is mostly applied only under ideal system voltage conditions to calculate the compensating currents. However, system voltage may not be balanced in industrial systems all the time. Under such conditions, control of the four-leg active power filter using the instantaneous reactive power theory does not result in the expected performance. The i_{d_axis}-i_{q_axis} current scheme is used to improve the active performance under non-ideal system voltage conditions (Montero et al., 2007; Suresh et al., 2011). The Synchronous Reference Frame (SRF) theory based algorithms are used for four-leg SAPF to compensate the current harmonics, reactive power and power factor improvement (Garcia Campanhol et al., 2014).

The Model Predictive Control (MPC) algorithm is used to predict the future behavior of the system by which control parameters are generated to get the desired output. The MPC system has several significant advantages:

- The control algorithms are easy and Intuitive.
- MPC control algorithm is suitable for variety of systems.
- A guaranteed stability is achieved by using the MPC based system. (Shekoofeh Jafari Fesharaki and Heidar Ali Talebi, 2014).
- MPC is a suitable and effective system for MIMO constrained linear systems. (Ebrahimi Bavili et al., 2015)
- An MPC algorithm with optimization process has the capability of controlling multi input, multi output (MIMO) nonlinear processes with better performance and prediction accuracy.(Germin Nisha and Pillai, 2015)
- Communication network with random time varying delay in control signals are effectively handled by the MPC with better performance. (Constantin and Corneliu Lazar, 2011)
- Number of system constraints can be included to perform a particular task.

This research paper presents model predictive current control algorithm for the four-leg shunt active power filter suitable for non-ideal system voltage and unbalanced non-linear load environment. Using the MPCC scheme, many major issues in controlling the SAPF, like regulation of DC bus voltage, low harmonic content in the input current during dynamic variation of input voltage, maximum output voltage of the inverter, current limitations are well addressed.

The main advantages of the proposed MPCC scheme in the SAPF are

- The proposed controller is capable of knowing the model of the plant for adjusting the controller parameters.
- Low harmonic content in input current during dynamic variation of input voltage
- Fast and dynamic control of control variables.
- The discrete time implementation which is useful in digital control platforms.
- Relatively simple control algorithm.

The compensating current generation is one of the important task to mitigate the current harmonics in the four-leg inverter based SAPF. The proposed system model predicts the value of the compensating current to be injected in advance for all possible voltage vectors generated by the four-leg inverter. The predictions are compared with the reference currents for each switching state and the error is found for each phase. The minimum error value (i.e.) predicted value is almost equal to the reference value, forms the cost function. The switching state corresponding to the cost function is applied at the next instant (Rodriguez and Cortes 2012). In the proposed MPCC controller the squared error is considered instead of absolute error, so that the cost function is reviewed for better accuracy and good reference tracking capability. This control model eliminates the task of controllers tuning and modulators. The principle advantage that the proposed MPCC control scheme offers over the other popularly used methods like Carrier based PWM and 3D Space vector modulation scheme are the following:

- The proposed MPCC controller considers the system to be non-linear, which is closer to real operating conditions whereas the conventional PI controller with carrier based PWM and/or 3D SVPWM technique adopts a linear system model to tune the controller.
- The optimized SAPF current controller is designed by using only a mathematical model of the system and not the conventional modulation stage and PI controller that has a bandwidth limitation. Such a limitation introduces significant error in the higher order component of current reference (Buso et al., 1998).
- Under dynamic variation of the system load currents, bus voltages and sudden switching of the SAPF, the proposed controller gives better performance.
- The proposed four-leg inverter based MPCC control gives a fast response with no overshoot as against the sluggish performance in terms of overshoot and response time (Gao Hanying et al., 2014; Sinsukthavorn et al., 2012).

Performances of the active power filter and the associated control scheme are validated through simulation results, and found that the practical implementation is feasible.

2. MATHEMATICAL MODEL OF FOUR-LEG INVERTER

The basic compensation principle of the shunt active power filter is shown in Fig. 1.

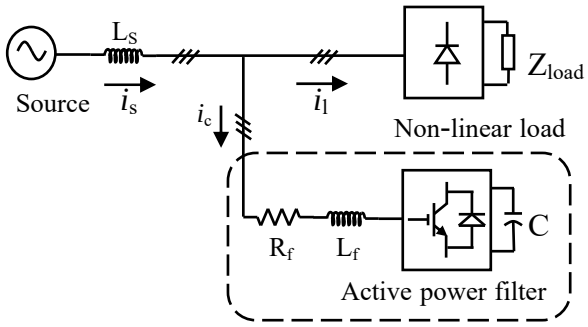

Fig. 1. Basic Compensation Principle of Shunt Active Power Filter.

A shunt active power filter is connected in parallel with the load. The control part of active power filter detects the harmonic current and estimates the required compensating current which is injected to mitigate the harmonic current. This results in a sinusoidal source current at the coupling point of the filter. The three-phase four-leg inverter with L filter as shown in Fig. 2 has additional two switches in the fourth leg.

The four-leg inverter has the following advantages compared to the conventional split-link inverter:

Provides path for neutral current through its fourth leg.

Less DC link capacitance and full utilization of DC link voltage.

Yields neutral point voltage control for supplying non-symmetrical and single phase loads.

The various switching states of the four-leg inverter and the corresponding voltage levels are presented in Table 1.

The voltage across any leg of the four-leg converter with respect to point 'N' can be expressed as,

$$\begin{aligned} V_{aN} &= S_a V_{dc} \\ V_{bN} &= S_b V_{dc} \\ V_{cN} &= S_c V_{dc} \\ V_{dN} &= S_d V_{dc} \end{aligned} \tag{1}$$

where V_{dc} and V_{dN} are DC link and load neutral voltages respectively, and S_a, S_b, S_c, S_d represent the switching state.

The outer phase-neutral voltages of the inverter are given by,

$$V_{jn} = \left[S_j - S_d\right] - V_{dc} \tag{2}$$

where j = a,b,c

Table 1. Switching States of Three-phase Four-leg inverter.

Switching State	$S_aS_bS_cS_n$	V_{aN}	V_{bN}	V_{cN}	V_{dN}	V_{ad}	V_{bd}	V_{cd}
1	1000	V_{dc}	0	0	0	V_{dc}	0	0
2	1100	V_{dc}	V_{dc}	0	0	V_{dc}	V_{dc}	0
3	0100	0	V_{dc}	0	0	0	V_{dc}	0
4	0110	0	V_{dc}	V_{dc}	0	0	V_{dc}	V_{dc}
5	0101	0	0	V_{dc}	0	0	0	V_{dc}
6	1010	V_{dc}	0	V_{dc}	0	V_{dc}	0	V_{dc}
7	1110	V_{dc}	V_{dc}	V_{dc}	0	V_{dc}	V_{dc}	V_{dc}
8	0000	0	0	0	0	0	0	0
9	1001	V_{dc}	0	0	V_{dc}	0	$-V_{dc}$	$-V_{dc}$
10	1101	V_{dc}	V_{dc}	0	V_{dc}	0	0	$-V_{dc}$
11	0101	0	V_{dc}	0	V_{dc}	$-V_{dc}$	0	$-V_{dc}$
12	0111	0	V_{dc}	V_{dc}	V_{dc}	$-V_{dc}$	0	0
13	0011	0	0	V_{dc}	V_{dc}	$-V_{dc}$	$-V_{dc}$	0
14	1011	V_{dc}	0	V_{dc}	V_{dc}	0	$-V_{dc}$	0
15	1111	V_{dc}	V_{dc}	V_{dc}	V_{dc}	0	0	0
16	0001	0	0	0	V_{dc}	$-V_{dc}$	$-V_{dc}$	$-V_{dc}$

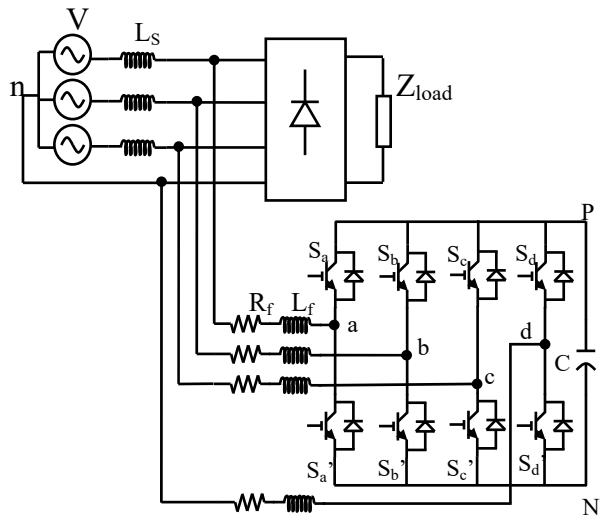

Fig. 2. Shunt Active Power Filter with Four-leg Inverter.

S_j is defined by,

$$S_j = \begin{cases} 1, & \text{if the upper switch of the leg is closed} \\ 0, & \text{if the upper switch of the leg is opened} \end{cases}$$

S_d is the corresponding switch state for neutral leg.

Equation (2) can also be re-written as,

$$\begin{bmatrix} V_{ad} \\ V_{bd} \\ V_{cd} \end{bmatrix} = \begin{bmatrix} 1 & 0 & 0 & -1 \\ 0 & 1 & 0 & -1 \\ 0 & 0 & 1 & -1 \end{bmatrix} \cdot \begin{bmatrix} S_a \\ S_b \\ S_c \\ S_d \end{bmatrix} . V_{dc} \tag{3}$$

By applying the Kirchhoff's voltage law, the inverter output voltages can be expressed as,

$$\begin{aligned} V_{aN} &= R_{fa} i_a + L_{fa} \frac{di_a}{dt} + V_{dN} \\ V_{bN} &= R_{fb} i_b + L_{fb} \frac{di_b}{dt} + V_{dN} \\ V_{cN} &= R_{fc} i_c + L_{fc} \frac{di_c}{dt} + V_{dN} \end{aligned} \tag{4}$$

where, R_{fa}, R_{fb} and R_{fc} are filter resistance of phase a, b and c respectively. L_{fa}, L_{fb}, and L_{fc} are filter inductance of phase a, b, and c respectively. i_a, i_b, and i_c are load current of phase a, b, and c respectively.

From (3) and (4), the load voltages are calculated as,

$$\begin{aligned} V_{ad} &= R_{fa} i_a + L_{fa} \frac{di_a}{dt} \\ V_{bd} &= R_{fb} i_b + L_{fb} \frac{di_b}{dt} \\ V_{cd} &= R_{fc} i_c + L_{fc} \frac{di_c}{dt} \end{aligned} \tag{5}$$

The change of output current vector can be obtained from Eqn. 5 as,

$$\frac{di_j}{dt} = \frac{V_{jd} - R_{fj} i_j}{L_{fj}} \tag{6}$$

where, j = a, b, c

A discrete time model is considered as sampling time is to be more important to obtain accurate results. A first-order approximation of the change in current described in Eqn. 6 can also be written as

$$\frac{di_j}{dt} = \frac{i_j(k) - i_j(k-1)}{T_s} \tag{7}$$

where, j = a, b, c

By substituting Eqn. 7 in Eqn. 6, the output current can be obtained as

$$i_j(k) = \frac{T_s V_j(k) + L_f i_j(k-1)}{L_{fj} + (R_{fj}) T_s} \tag{8}$$

where, j = a, b, c

The system in Eqn. 4 can be represented in state-space form as,

$$\begin{aligned} \dot{x} &= Ax + Bu \\ y &= Cx \end{aligned} \tag{9}$$

where

$$x = [x_1 \quad x_2 \quad x_3]^T = [i_a \quad i_b \quad i_c]^T$$

$$u = [u_1 \quad u_2 \quad u_3]^T = [V_{ad} \quad V_{bd} \quad V_{cd}]^T$$

$$A = \begin{bmatrix} -\frac{R_{fa}}{L_{fa}} + \frac{L_{eq}}{L_{fa}}\left(\frac{R_{fa}}{L_{fa}} - \frac{R_{fn}}{L_{fn}}\right) & \frac{L_{eq}}{L_{fa}}\left(\frac{R_{fb}}{L_{fb}} - \frac{R_{fn}}{L_{fn}}\right) & \frac{L_{eq}}{L_{fa}}\left(\frac{R_{fc}}{L_{fc}} - \frac{R_{fn}}{L_{fn}}\right) \\ \frac{L_{eq}}{L_{fb}}\left(\frac{R_{fa}}{L_{fa}} - \frac{R_{fn}}{L_{fn}}\right) & -\frac{R_{fb}}{L_{fb}} + \frac{L_{eq}}{L_{fb}}\left(\frac{R_{fb}}{L_{fb}} - \frac{R_{fn}}{L_{fn}}\right) & \frac{L_{eq}}{L_{fb}}\left(\frac{R_{fc}}{L_{fc}} - \frac{R_{fn}}{L_{fn}}\right) \\ \frac{L_{eq}}{L_{fc}}\left(\frac{R_{fa}}{L_{fa}} - \frac{R_{fn}}{L_{fn}}\right) & \frac{L_{eq}}{L_{fc}}\left(\frac{R_{fb}}{L_{fb}} - \frac{R_{fn}}{L_{fn}}\right) & -\frac{R_{fc}}{L_{fc}} + \frac{L_{eq}}{L_{fc}}\left(\frac{R_{fc}}{L_{fc}} - \frac{R_{fn}}{L_{fn}}\right) \end{bmatrix}$$

$$B = \begin{bmatrix} \frac{1}{L_{fa}}\left(1 - \frac{L_{eq}}{L_{fa}}\right) & -\frac{1}{L_{fa}}\frac{L_{eq}}{L_{fb}} & -\frac{1}{L_{fa}}\frac{L_{eq}}{L_{fc}} \\ -\frac{1}{L_{fb}}\frac{L_{eq}}{L_{fa}} & \frac{1}{L_{fb}}\left(1 - \frac{L_{eq}}{L_{fb}}\right) & -\frac{1}{L_{fb}}\frac{L_{eq}}{L_{fc}} \\ -\frac{1}{L_{fc}}\frac{L_{eq}}{L_{fa}} & -\frac{1}{L_{fc}}\frac{L_{eq}}{L_{fb}} & \frac{1}{L_{fc}}\left(1 - \frac{L_{eq}}{L_{fc}}\right) \end{bmatrix}$$

$$C = \begin{bmatrix} 1 & 0 & 0 \\ 0 & 1 & 0 \\ 0 & 0 & 1 \end{bmatrix}$$

$$L_{eq} = \left(\frac{1}{L_{fa}} + \frac{1}{L_{fb}} + \frac{1}{L_{fc}} + \frac{1}{L_{fd}}\right)^{-1}$$

The block diagram of the mathematical model in Eqn. 9 is shown in Fig. 3.

3. COMPENSATING CURRENT REFERENCE GENERATION

The reference signal for each phase compensating current is obtained from the harmonic component of the corresponding load current. The proposed model predictive current control utilizes the i_{d_axis}-i_{q_axis} current method (Tepper et al., 1996; Soares et al., 1997). The most important characteristics of

this method is that the compensation current calculation does not involve the source voltage. Hence, this control method achieves a superior harmonic compensation and performance under distorted system voltage. The i_{d_axis}-i_{q_axis} control method is based on a synchronous rotating frame obtained from the park's transformation. The load currents are measured and the transformation is applied to obtain the i_{d_axis} and i_{q_axis} current component. The reference signal for the compensating current generation scheme is shown in Fig. 4.

By using Park's transformation, the i_{d_axis}, i_{q_axis} and i_{o_axis} current components are estimated. A low-pass filter extracts the DC component of the line current (i_{d_axis}) is used as reference component for harmonic compensation. The reactive reference component of the line current is obtained by inverting the corresponding line current components of i_{q_axis}. The i_{o_axis} current component can be fed as such, to control the zero-sequence harmonics. The resulting i_{d_axis} signal, together with i_{q_axis} and i_{o_axis} are transformed back into a three-phase system by the inverse Park's transformation. The instantaneous current that flows through the neutral line is compensated by using the instantaneous sum and opposite magnitude of the three phase currents.

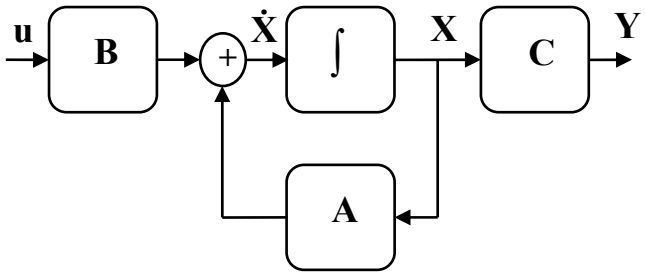

Fig. 3. Block Diagram of State-space model of the System.

4. MODEL PREDICTIVE CURRENT CONTROL

Model Predictive Current Control is an advanced method of control scheme used in the field of power electronics and industrial drives. The dynamic control response for various operating limits is its inherent advantage. The four-leg inverter switching states are discretized to develop the Finite Control Set (FCS) model predictive control. Since the four-leg inverter has a finite number of switching states, the predictions and optimizations are greatly simplified for the proposed MPCC technique. Moreover, this system does not require internal current control loops and modulators, resulting in less computational complexity.

The control method of FCS-MPCC predicts the load current in advance for each valid switching state of the converter. From Eqn. 6 and Table 1, it is clear that the load current and predicted load voltage vary in each switching state. The predicted current is compared with the reference current value to calculate the error. The error for each phase is calculated and added up and the squared value of the error is used for precise tracking. Similarly, the error is repeatedly found in all the possible switching states. The minimum error value is the cost function and the corresponding switching state of that cost function is applied at the end of each sampling time.

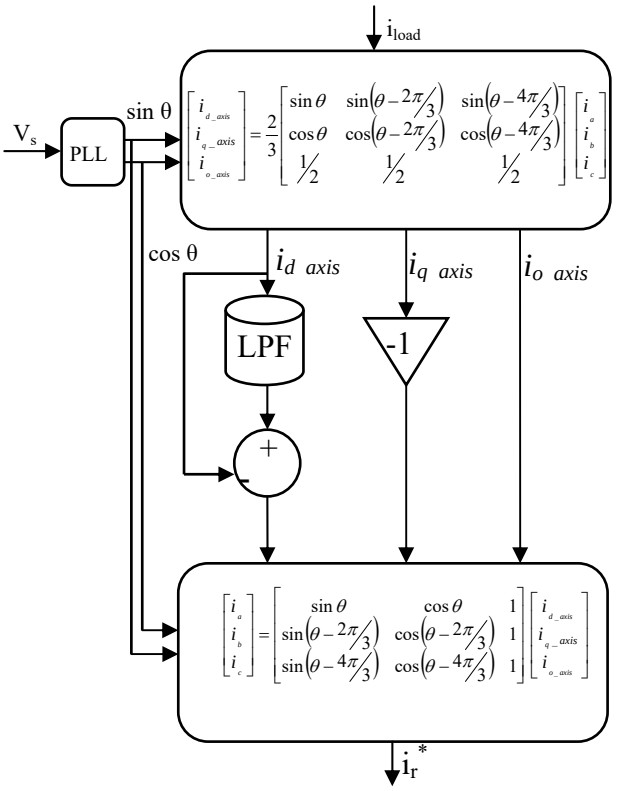

Fig. 4. Generation of Reference Signal for Compensating Current.

The implementation of model predictive control shown in Fig. 5 requires the following steps:

a) Definition of the mathematical model of four-leg inverter

b) Measurement and error calculation

c) Optimization of the cost function

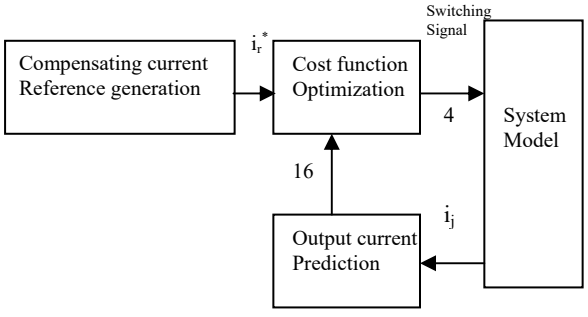

Fig. 5. Model for Predictive Current Control System.

4.1 Modeling of Four-Leg Inverter

The state-space model of four-leg inverter shown in Fig. 3 is considered to implement the proposed MPCC. The output current is predicted by finding the state transition matrix for the state-space model. The significance of finding the state

transition matrix is to get the response of the system for initial conditions and for other variations (Kuo, 2002). It consists of two components,

1) A free response component (for initial conditions only) given by J

2) A forced response component given by K

The output current prediction requires the value of the load current and the load voltage, for various switching states. The algorithm calculates all possible conditions that the state variables can achieve for all the 16 switching states. The recursive equation of the system is given by,

$$i[k+n+1] = \boldsymbol{J}\, i[k+n] + \boldsymbol{K}\, V[k+n],\ n = 0,1,2,.$$

where,

$$J = \begin{bmatrix} j_1 & j_2 & j_3 \\ j_4 & j_5 & j_6 \\ j_7 & j_8 & j_9 \end{bmatrix} = e^{AT_S}$$
$$K = \begin{bmatrix} k_1 & k_2 & k_3 \\ k_4 & k_5 & k_6 \\ k_7 & k_8 & k_9 \end{bmatrix} = A^{-1}(J - C)B \qquad (10)$$

4.2 Error Calculation

The compensating current reference is measured and the output currents $i_j(k+1)$ are predicted with the help of the system model shown in Fig. 4. The state transition equation given in Eqn. 10 has complex matrix calculation. Therefore, the calculations are done separately by using mathematical tools and the parameters *J* and *K* are initialized beforehand. The measured reference currents, $i_r^*(k+1)$, are compared with their predicted values and the error is calculated. The errors obtained for all the three phases are added and then squared.

$$w = \left\| i_r^*(k+1) - \left[i_a(k+1) + i_b(k+1) + i_c(k+1) + i_d(k+1) \right] \right\|^2 \qquad (11)$$

4.3 Cost Function Optimization

In the model predictive control scheme the several control targets, variables, and constraints can be included in a single cost function and simultaneously controlled. In this paper, the control target is considered to optimize the current error. The error (*w*) is calculated for all the switching states (i.e.) 16 switching states.

The cost function, *cf* is obtained from the minimum value of *w*. The output current equals its reference current when *cf* = 0. The minimum cost function value near to zero is selected and the corresponding switching state is applied to the four-leg inverter switches at the end of each sampling instant. The voltage vector $V_j(k+1)$ for the minimum cost function is used for the succeeding step to predict the current in advance. Thus, at k^{th} instant, the algorithm selects a switching state, which would generate an accurate current value close to the reference value. This minimizes the cost function at the *k+1* instant, and then optimal switching state is applied during the entire (*k+1*) period. The predictive current control algorithm shown in Fig. 6 has been implemented using MATLAB S-function block. This S-function block is used to operate with a discrete update method at the sample time, T_s defined for the predictive algorithm. The process of measuring, optimizing the cost function, and finding the optimal switching state is completed using the update method available in S-function to generate the switching states at the end of k^{th} instant.

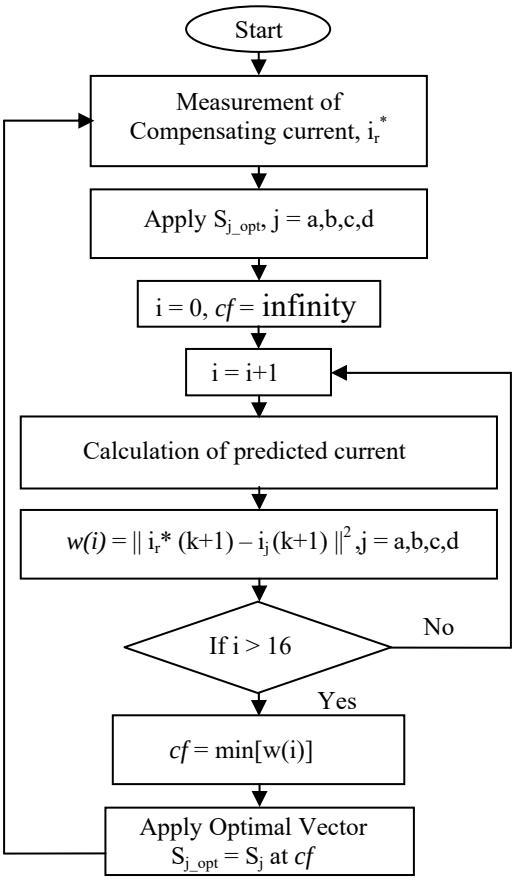

Fig. 6. The Flow Diagram of Predictive Current Control Algorithm.

5. SIMULATION RESULTS AND DISCUSSION

In order to verify the proposed control technique, to achieve the main objective for the three-phase four-wire system with shunt active power filter, the system is simulated using MATLAB/Simulink. The extensive simulation studies are carried out using the system parameters given in Table 2. The frequency of output voltage and current are found to be much lesser compared to the sampling frequency, so that the system voltage does not change considerably for each sampling instant. Therefore, the switching frequency always be less than the sampling frequency (Rodriguez and Cortes, 2012). In fact, the switching state of the inverter can be changed only once during each sampling instant, thus switching frequency is limited to half the sampling frequency. However, switching states do not change in every sampling

instant; therefore, the average switching frequency is always less. The main objective of the system is considered as

- Balancing of the three-phase currents with sinusoidal nature
- Zero current in the system neutral

Table 2. Specification for Shunt Active Power Filter.

Symbol	Parameter	Values
S	Apparent Power	10 kVA
V_s	Supply Phase Voltage	240 V
V_{dc}	DC Link Voltage	650 V
R	Load Resistance	50 Ω
L	Load Inductance	12 mH
L_s	Line Impedance	2.3 mH
L_f	Filter Inductance	5 mH
R_f	Filter Resistance	0.5 Ω
T_s	Sampling Time	20 µs

To show the effectiveness of the proposed control in the shunt active power filter, the simulation studies are carried out for the following operating conditions:

- Balanced load conditions
- Unbalanced load conditions
- Unbalanced system voltage
- Dynamic switching of SAPF

Under all operating conditions, the effectiveness of the proposed control scheme is verified using the source current waveform and the corresponding THD spectrum.

5.1 Case A: Balanced load condition

In the first case, the shunt active power filter with the proposed controller is simulated for balanced three-phase non-linear loads. The loads are considered as a three-phase diode bridge rectifier with RL load and three single-phase diode bridge rectifiers with RL load. The load current, compensating current, compensated source current and neutral current waveforms are presented in Fig. 7. In addition to the reference tracking capabilities of the control method, another important performance parameter of the shunt active filter is the source current THD value. To show the effectiveness of the SAPF, the THD spectrum of source and load current are analyzed. The Fig. 8 and Fig. 9 show the THD spectrum of source and load current respectively, and the THD value is found to be reduced from 18.29% to 3.58%. As the controller is not limited to fixed switching frequency, it is found that the harmonic frequencies are found in all scales. However, the harmonic magnitude level is found to be low in all scales of frequency (IEEE Std 519, 1992). The source current is also retained to its sinusoidal nature.

5.2 Case B: Unbalanced load condition

In the second case, the trial system is simulated for unbalanced load condition. Three single-phase rectifiers are connected to each phase along with a three-phase rectifier load. At time t = 0.1 s, the two single phase rectifier load in phase B and phase C is disconnected to give unbalanced load condition. Thus, the controller shows robustness for load parameter variations. It can be seen from Fig. 10 that the change in load has not affected the behavior of the control system and a balanced supply is also maintained ensuring no effect on three phase rectifier load. The unbalanced current flow is controlled through the neutral leg to the load.

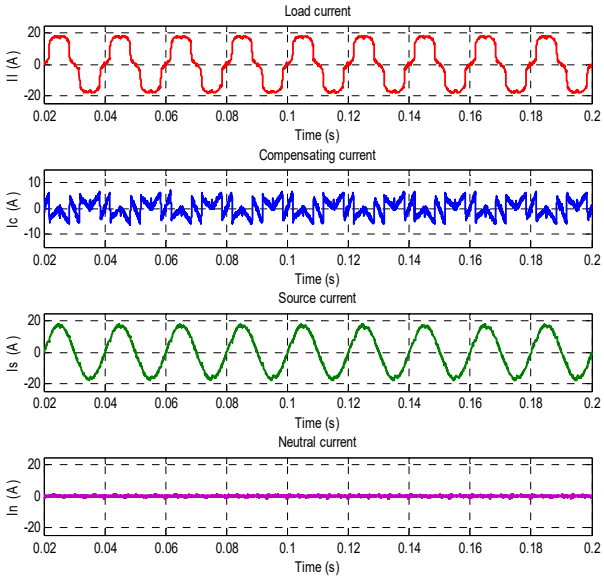

Fig. 7. Current Waveforms of SAPF for Balanced Load Condition.

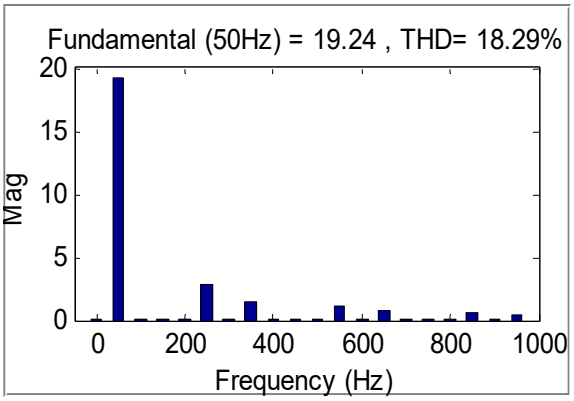

Fig. 8. THD Spectrum of Load Current .

5.3 Case C: Unbalanced system voltage

In the third case, the test system is simulated for unbalanced system voltage. The Phase A is considered as an unbalanced phase voltage of 200 V and the resultant current waveforms are presented in Fig. 11. It can be seen that, the source current is balanced under unbalanced source voltage conditions. This shows that the performance of the three-phase load is not affected by the system condition. The system is also simulated for unbalanced load with the unbalanced system voltage condition. The corresponding unbalanced source voltage, unbalanced load current, and the balanced source

current waveforms are shown in Fig. 11. The results prove that the robustness of the controller under unbalanced condition of both load and source.

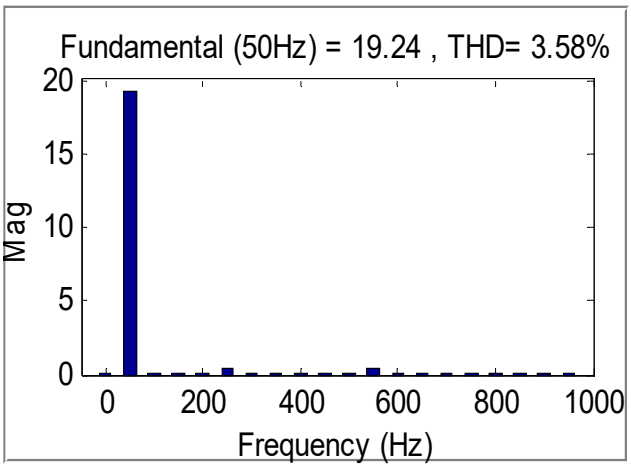

Fig. 9. THD Spectrum of Source Current with SAPF.

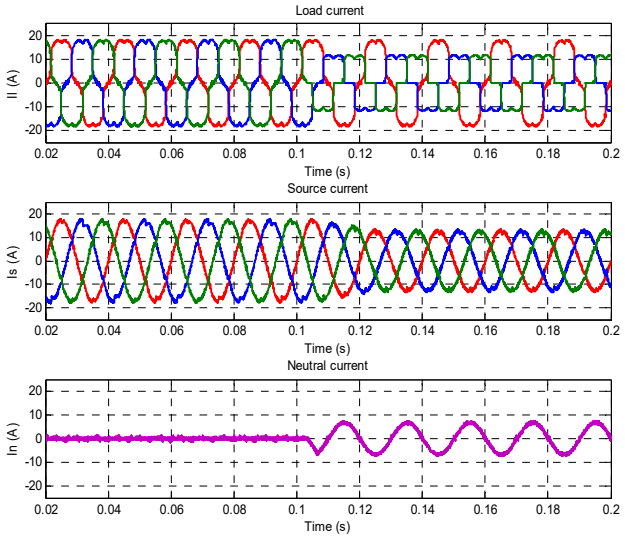

Fig. 10. Current Waveforms of SAPF for Unbalanced Load Condition.

5.4 Case D: Dynamic performance

In the fourth case to show, the system performance under dynamic condition, the trial system is simulated for sudden connection of the shunt active power filter with the arrangement. The shunt active power filter is a non-linear model; therefore, compensation effectiveness as well as transient response depends on how accurate the associated developed linear model. The Fig. 12 shows the three phase compensating current reference and its associated compensating current. It proves that the effectiveness of the proposed model is under transient condition. There is no overshoot observed in the controller during transient conditions. Fig. 13 shows the current waveforms of load current, compensating current and source current, when the SAPF is connected to the system. It can be seen that, the performance of the controller under such dynamic conditions has not affected the system.

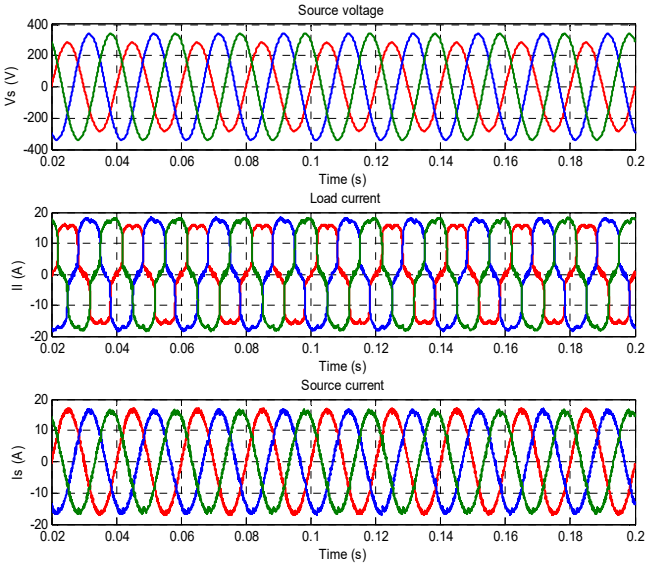

Fig. 11. Current Waveforms of SAPF for Unbalanced System Voltage Condition.

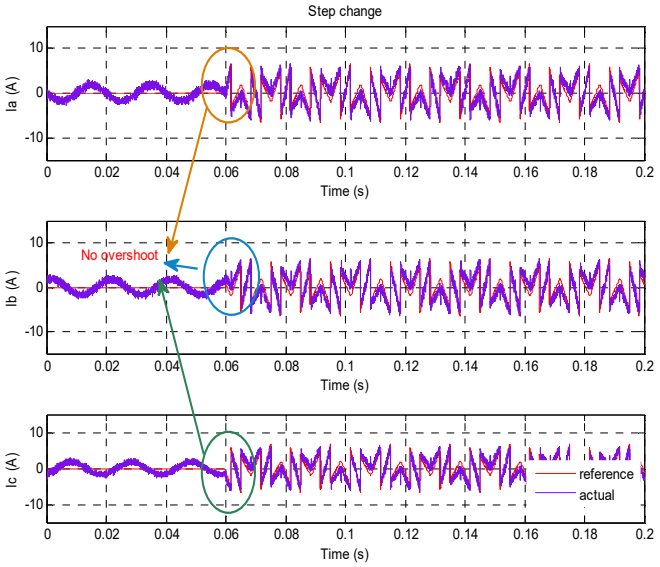

Fig. 12. Current Waveforms under Dynamic Switching of SAPF using Predictive Control.

The SAPF is a type of non-linear model and the response of the predictive control shows robust performance when compared to Proportional Integral (PI) controllers as PI controllers are more suitable for linear load. As shown in Fig. 12, it can be seen that, predictive control has good tracking capability even during transient conditions, whereas the PI controller being a linear modulator does not withstand good transient behavior. The performance of the PI controllers depends on the appropriate adjustment of the parameters K_p and K_i. In the predictive control scheme, there are no parameters to adjust, but a cost function must be defined, which in the case of current control is very simple. The PI controller works along with a modulator, so that the necessary switching interval can be obtained. This stage is not needed in the predictive control scheme as the switching states are generated directly by the controller.

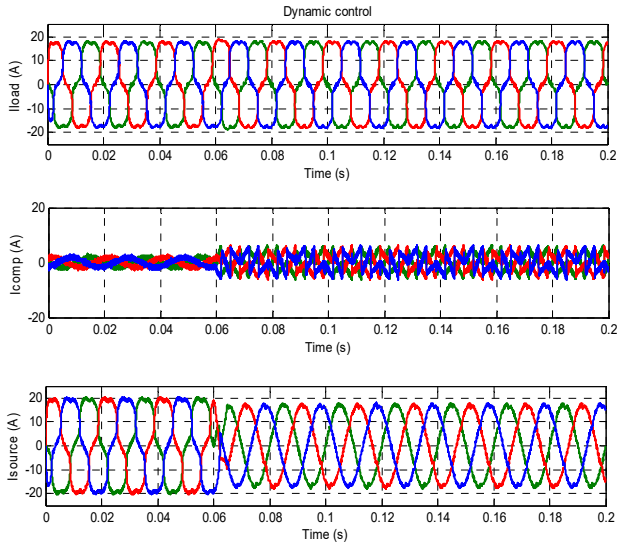

Fig. 13. Controller Performance of SAPF using Predictive Control.

The simulation results reveal that the proposed four leg shunt active power filter topology with MPCC control can play a vital role in the following applications:

- A distribution system with non-linear and unbalanced single phase loads leads the neutral loading, harmonics, unbalanced currents and poor power factor (Igor Musulin and ŽeljkoJakopović, 2013). To balance the three-phase load currents and to improve the power quality, the proposed four-leg SAPF with MPCC control provides a good solution.

- Recently, Renewable energy supply found increasing in the existing grid system. (Mukhtiar Singh et al., 2011). In such distributed generation system, non symmetrical voltage problem is one of the frequent power quality issues, especially in islanding modes of operation, which can be effectively eliminated using the proposed system.

- To maximize the utilization of the existing transmission line, improve the voltage profile and to increase the stability limit, Flexible AC Transmission System (FACTS) provides a good solution. Four leg inverter topology based FACTS devices like STATCOM, and DVR (Tashackori et al., 2013) with the proposed MPCC controller can provide an improved solution under all dynamic conditions.

6. CONCLUSION

This paper has presented the use of a shunt active power filter for compensating source current harmonics with the proposed predictive current control technique. This technique does not require internal current control loop and modulator and therefore involves less computational complexity. The proposed predictive control results in better dynamic performance, good reference tracking and the ability to control a non-linear model (SAPF). The shape of the source side current is found to be sustained sinusoidal similar to the source voltage shape. In addition, the unbalanced load conditions do not affect the distribution system due to control over the flow of neutral current in the load side. Simulated results validated the performance of the predictive current controller in SAPF, and the source current THD is found to have reduced from 18.29% to 3.58%, which is well within the IEEE-519 standard.

REFERENCES

Acordi, E.J. da Silva, I.N. and Machado, R.Q. (2014). Application of fuzzy systems in the control of a shunt active power filter with four-leg topology. In: *International Joint Conference on Neural Networks IJCNN 2014*. pp.1239-1244.

Akagi, H., Kanazawa, Y. and Nabae, A. (1984). Instantaneous Reactive Power Compensators Comprising Switching Devices without Energy Storage Components. *IEEE Transactions on Industry Applications*, IA-20(3), pp.625-630.

Aredes, M., Hafner, J. and Heumann, K. (1997). Three-phase four-wire shunt active filter control strategies. *IEEE Transactions on Power Electronics*, 12(2), pp.311-318.

Buso, S. Malesani, L. and Mattavelli, P. (1998) Comparison of current control techniques for active filter applications. In: *IEEE Transactions on Industrial Electronics*. 45(5). pp.722-729.

Constantin F. Caruntu and Corneliu Lazar. (2011). Networked Predictive Control for Time-varying Delay Compensation with an Application to Automotive Mechatronic Systems. *Control Engineering and Applied Informatics,* 13(4), pp. 19-25.

Ebrahimi Bavili, R. Khosrowjerdi, M. J. and Vatankhah, R. (2015). Active Fault Tolerant Controller Design using Model Predictive Control. *Control Engineering and Applied Informatics,* 17(3), pp. 68-76.

Ei-Barbari S., and Hofmann, W. (2000). Digital control of a four leg inverter for standalone photovoltaic systems with unbalanced load. In: *Industrial Electronics Society, 2000. IECON 2000*. Nagoya: IEEE, pp.729-734.

Enjeti, P., Shireen, W. Packebush, P. and Pitel, I. (1994). Analysis and Design of a New Active Power Filter to Cancel Neutral Current Harmonics in Three-Phase Four-Wire Electric Distribution Systems. *IEEE Transactions on Industry Applications*, 30(6), pp.1565-1571.

Fernandes, D.A., Costa, F.F., Vitorino, M.A., Queiroz K.I.P.M., and Salvadori, F. (2013). Carrier-based PWM scheme for three-phase four-leg inverters. In: *Industrial Electronics Society, IECON 2013*. IEEE, pp.3353 - 3358.

Gao Hanying. Zhang Momo. Chen Kai. and Zhang Tianyu. (2014) Study on three-phase four-leg PMSM control system. In: *IEEE Conference and Expo Transportation Electrification* Asia-Pacific. ITEC Asia-Pacific. pp.1-6.

Garcia Campanhol, L. B. Oliveira da Silva, S.A. and Goedtel, A. (2014) Application of shunt active power filter for harmonic reduction and reactive power compensation in three-phase four-wire systems. In: *IET Power Electronics*, 7(11). pp.2825-2836.

Germin Nisha, M and Pillai, G. N. (2015). Nonlinear model predictive control of MIMO system with Least squares support vector machines and Particle swarm

optimization. *Control Engineering and Applied Informatics,* 17(4), pp. 14-22.

IEEE Std 519-1992, (1992). IEEE Recommended Practices and Requirements for Harmonic Control in Electrical Power Systems. pp.1-112.

Igor Musulin and ŽeljkoJakopović. (2013). Three-Phase Inverters Supplying Non-Symmetrical, Non-Linear and Single Phase Loads. In: *International Conference on Electrical Drives and Power Electronics*, EDPE 2013, Dubrovnik, Croatia, pp.184-191.

Joshi, T.G.S. Kumar, A.S. Joseph, A. and Unnikrishnan, A. K. (2012) Four-leg active filter based solution to IT Park's power quality issues. In: *International Conference on Power Electronics, Drives and Energy Systems PEDES. IEEE*. pp.1-6.

Khadkikar, V. Chandra, A. and Singh, B. (2011). Digital signal processor implementation and performance evaluation of split capacitor, four-leg and three H-bridge-based three-phase four-wire shunt active filters. *IET Power Electronics*, 4(4), p.463-470.

Kuo, B. (2002). *Automatic control systems*. 8th ed. New York, NY, USA: John Wiley & Sons, Inc.

Montero, M. Cadaval, E. and Gonzalez, F. (2007). Comparison of Control Strategies for Shunt Active Power Filters in Three-Phase Four-Wire Systems. *IEEE Transactions on Power Electronics*, 22(1), pp.229-236.

Mukhtiar Singh, Ambrish Chandra, Rajiv, K. Varma.(2011) Grid Interconnection of Renewable Energy Sources at the Distribution Level With Power-Quality Improvement Features. *IEEE Transactions On Power Delivery*, 26(1), p.307-315.

Nguyen-Van Nho, Myung-Bok Kim, Gun-Woo Moon, and Myung-Joong Youn, (2004). A novel carrier based PWM method in three phase four wire inverters. In: *Industrial Electronics Society, 2004. IECON 2004.*. IEEE, pp.1458 - 1462.

Quinn C.A. Mohan, N. and Mehta, H. (1993). A Four-Wire Current Controlled Converter Provides Harmonic Neutralisation in Three-Phase-Four Wire Systems. In: *Applied Power Electronics Conference and Exposition*. San Diego, CA: IEEE, pp.841 - 846.

Rodriguez, J. and Cortes, P. (2012). *Predictive control of power converters and electrical drives*. Chichester, West Sussex, UK: Wiley.

Shekoofeh Jafari Fesharaki, Heidar Ali Talebi. (2014). Active Front Steering Using Stable Model Predictive Control Approach via LMI. *Control Engineering and Applied Informatics,* 16(2), pp. 90-97.

Singh, B., Ai-Haddad, K. and Chandra, A. (1998). Active power filters for harmonic and reactive power compensation in three-phase, four-wire systems supplying non-linear loads. *European Transactions on Electrical Power*, 8(2), pp.139-145.

Sinsukthavorn, W. Ortjohann, E. Mohd, A. Hamsic, N. and Morton, D. (2012). Control Strategy for Three-/Four-Wire-Inverter-Based Distributed Generation. In: *IEEE Transactions on Industrial Electronics*.59 (10). Pp-3890-3899.

Soares, V. Verdelho, P. and Marques G. (1997). Active power filter control circuit based on the instantaneous active and reactive current id-iq method. In: *Power Electronics Specialists Conference, 1997. PESC '97*. St. Louis, MO: IEEE, pp.1096 - 1101.

Suresh, M. Patnaik, S.S. Suresh, Y. and Panda, A.K.(2011) Comparison of two compensation control strategies for shunt active power filter in three-phase four-wire system. In: *Innovative Smart Grid Technologies ISGT 2011, IEEE PES* . pp.1-6.

Tashackori, A. Hosseini, S.H. Sabahi, M. and Nouri, T. (2013). A three-phase four-leg DVR using three dimensional space vector modulation. In: *21st Iranian Conference on Electrical Engineering ICEE*. pp.1-5.

Tepper, J., Dixon, J., Venegas, G. and Moran, L. (1996). A simple frequency-independent method for calculating the reactive and harmonic current in a nonlinear load. *IEEE Transactions on Industrial Electronics*, 43(6), pp.647-654.

Verdelho, P. and Marques, G. (1997). An active power filter and unbalanced current compensator. *IEEE Transactions on Industrial Electronics*, 44(3), pp.321-328.